Science of the Total Environment 880 (2023) 163236

Contents lists available at ScienceDirect

Science of the Total Environment

journal homepage: www.elsevier.com/locate/scitotenv

Mechanisms underlying the responses of microbial carbon and nitrogen use efficiencies to nitrogen addition are mediated by topography in a subtropical forest

Xinyi Yang [a,b], Pengpeng Duan [a,b], Lettice Hicks [c], Kelin Wang [a,b], Dejun Li [a,b,*]

[a] Key Laboratory of Agro-Ecological Processes in Subtropical Region, Institute of Subtropical Agriculture, Chinese Academy of Sciences, Changsha 410125, China
[b] Guangxi Key Laboratory of Karst Ecological Processes and Services, Huanjiang Observation and Research Station for Karst Ecosystems, Institute of Subtropical Agriculture, Chinese Academy of Sciences, Huanjiang 547100, China
[c] Section of Microbial Ecology, Department of Biology, Lund University, Lund 223 62, Sweden

HIGHLIGHTS

- Microbial CUE and NUE increased under N addition at both topographic positions.
- Soil C and N cycles were decoupled by N addition in the valley.
- Microbial community and substrate availability regulated CUE and NUE in the valley.
- Soil P availability was a key driver regulating microbial CUE and NUE on the slope.

GRAPHICAL ABSTRACT

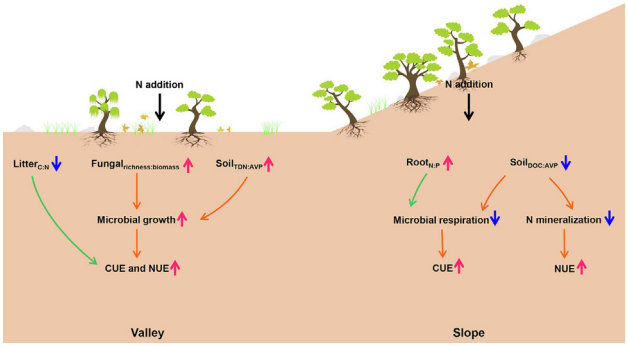

ARTICLE INFO

Editor: Manuel Esteban Lucas-Borja

Keywords:
Nitrogen deposition
Topography
Microbial carbon use efficiency
Microbial nitrogen use efficiency
Karst forest

ABSTRACT

Microbial carbon use efficiency (CUE) and nitrogen use efficiency (NUE) are key parameters determining the fate of C and N in soils. Atmospheric N deposition has been found to heavily impact multiple soil C and N transformations, but we lack understanding of the responses of CUE and NUE to N deposition, and it remains uncertain whether responses may be mediated by topography. Here, a N addition experiment with three treatment levels (0, 50 and 100 kg N ha^{-1} yr^{-1}) was conducted in the valley and on the slope of a subtropical karst forest. Nitrogen addition increased microbial CUE and NUE at both topographic positions, but the underlying mechanisms differed. In the valley, the increase in CUE was associated with an increase in soil fungal richness:biomass and lower litter C:N, whereas on the slope, the response was linked with a reduced ratio of dissolved soil organic C (DOC) to available phosphorus (AVP) which reduced respiration, and increased root N:P stoichiometry. In the valley, the increase in NUE was explained by stimulated microbial N growth relative to gross N mineralization, which was associated with increased ratios of soil total dissolved N:AVP and fungal richness:biomass. In contrast, on the slope, the increase in NUE was attributed to reduced gross N mineralization, linked to increased DOC:AVP. Overall, our results highlight how topography-driven soil substrate availability and microbial properties can regulate microbial CUE and NUE.

* Corresponding author at: Key Laboratory of Agro-Ecological Processes in Subtropical Region, Institute of Subtropical Agriculture, Chinese Academy of Sciences, Changsha 410125, China.
E-mail address: dejunli@isa.ac.cn (D. Li).

http://dx.doi.org/10.1016/j.scitotenv.2023.163236
Received 16 January 2023; Received in revised form 14 March 2023; Accepted 29 March 2023
Available online 6 April 2023

1. Introduction

Microbial carbon use efficiency (CUE) and nitrogen use efficiency (NUE) are important parameters influencing the fate of organic C and N in soils (Spohn et al., 2016b; Zhang et al., 2019). Microbial CUE (or NUE) describes the proportion of C (or N) allocated to growth relative to total microbial C (or N) uptake, with that not used for growth released into the environment through microbial respiration (or N mineralization) (Mooshammer et al., 2014; Fuchslueger et al., 2019). As such, microbial CUE and NUE reflect the capacity of C and N to be retained in the soil (Manzoni et al., 2012), as C and N used to build new microbial biomass may be more effectively stabilized in soil (Liang et al., 2017; Buckeridge et al., 2020). While the role of microbial CUE in regulating soil C sequestration and loss has been widely studied, there are far fewer assessments of microbial NUE. A more comprehensive evaluation of the factors controlling CUE and NUE is therefore crucial to improve projections of soil C and N cycling at the landscape scale.

Substrate stoichiometry has been demonstrated to be important in controlling CUE and NUE by affecting microbial investment in enzymes for resource acquisition (Zhang et al., 2019; Li et al., 2021a). According to the theory of stoichiometric homeostasis, a higher soil C:N ratio is usually linked to lower CUE and higher NUE as microorganisms need to maintain their homeostatic C:N balance through overflow respiration and investment of C into enzymes for nutrient acquisition (Feng et al., 2021). In contrast, where the C:N in soil is lower, decomposers conserve C and liberate excess N via mineralization, so they are expected to reduce their NUE while increasing CUE (Mooshammer et al., 2014).

Microbial CUE and NUE are community characteristics, and thus represent an integration of the activities of different microbial assemblages, and reflect the complex interactions between microbial community composition and the stoichiometry of available resources (Preusser et al., 2017). Indeed, CUE appears to be partially phylogenetically constrained (Hasby et al., 2021; Smith et al., 2021), suggesting that different communities may give rise to differences in microbial CUE. For example, Domeignoz-Horta et al. (2020) found that a shift in bacterial community was associated with a change in CUE, with CUE being positively associated with bacterial diversity whereas there was no correlation between fungal diversity and CUE. However, other studies have found the relationship between microbial diversity and CUE to be neutral (Malik et al., 2018) or negative (Zhang et al., 2020). In a managed grassland, a lower fungi:bacteria biomass was linked with a higher microbial CUE, but there was no clear relationship with NUE (Fuchslueger et al., 2019). Different microbial strains may vary in their metabolic activity (Kamble and Bååth, 2016; Cheng et al., 2017), with fungal communities often being characterized by a higher microbial CUE relative to bacterial communities (Gavazov et al., 2022). Moreover, fungi communities are dominant in secreting enzymes that degrade organic matter (Bonner et al., 2018), which in turn consume C and N, and may thus decrease microbial CUE and NUE. As microbial community structure is tightly associated with the quantity and quality of substrate use in soils (Zhang et al., 2018), changes in microbial community composition and diversity via changes in the abiotic environment (e.g., resource limitation and availability) may impact microbial CUE and NUE. Elevated atmospheric N deposition can impact soil resource availability, and microbial community abundance and composition which in turn may influence microbial metabolism (Bonner et al., 2018; Li et al., 2021b). For instance, a 6-year N addition resulted in a higher soil microbial CUE as a consequence of enhanced microbial growth in an alpine steppe (Feng et al., 2022). In a temperate forest, N addition increased microbial NUE in the organic layer of a forest by enhancing microbial N uptake and decreasing gross N mineralization; fungal community structure was positively correlated with microbial CUE in the organic soil layer, while bacterial community structure was positively associated with both CUE and NUE in the mineral soil layer after N addition (Li et al., 2021b). Nevertheless, how substrate availability as well as microbial community composition simultaneously affect microbial CUE and NUE remains unclear.

Topography has been found to substantially affect soil C and nutrient availability (Viscarra Rossel et al., 2019), thereby affecting the stoichiometry of substrates (Yuan et al., 2020), and subsequently soil microbial or enzyme activities, microbial community abundance and composition (Du et al., 2015; Fairbanks et al., 2020). For example, soil enzyme activities were lower in the valley than on the slope in a mountainous coniferous forest (Keller et al., 2023). Topography can also impact the fate of atmospherically deposited N, thereby impacting soil N status, and resulting in different responses of microbes to N addition between the valley and ridge (Enanga et al., 2017; Zhu et al., 2021).

In the current study, we proposed a conceptual framework linking substrate stoichiometry, plant detritus inputs and the microbial community to the responses of microbial metabolism to N addition (Fig. S1). We expected that N addition would directly increase soil N availability, and result in the alteration of soil C:N:P stoichiometry (Cheng et al., 2014), and microbial community abundance or composition (Zhang et al., 2018), which would subsequently stimulate or inhibit gross N mineralization, microbial respiration and microbial growth rates (Eastman et al., 2021; Ning et al., 2021). This would, in turn, determine the microbial CUE and NUE (Yuan et al., 2019; Li et al., 2021b; Feng et al., 2022). Meanwhile, N addition often promotes plant productivity and thus increases plant detritus inputs, which in turn increases available substrates for microbes (Zhang et al., 2018; Wu et al., 2022), and affects microbial community composition (Preusser et al., 2017). To test the above framework, we conducted a field N addition experiment to explore the responses and associated drivers of microbial CUE and NUE to elevated N addition in the valley and on the slope of a subtropical karst forest. Previous studies have shown that N addition decreased C:N and increased N:P in soil, which may strengthen microbial C and P limitations (Duan et al., 2022b; Yang et al., 2023). We therefore hypothesized that (1) N addition would increase microbial demand for C, thereby increasing microbial CUE. Moreover, our previous work at the studied subtropical karst forest has shown that soil N concentrations are higher on the slope than in the valley (Duan et al., 2022a), and that N addition inhibited biological N_2 fixation in the valley but not on the slope (Wang et al., 2019). We therefore hypothesized that (2) N addition would have a more pronounced effect on microbial metabolic activity in the valley by alleviating microbial N limitation, and thereby reducing microbial NUE.

2. Materials and methods

2.1. Site description and experimental design

The study was carried out in a humid subtropical karst forest, located in the Mulun National Nature Reserve, southwest China (Duan et al., 2022a; Duan et al., 2022c; Yang et al., 2023). The atmospheric N deposition rate in the region is 37 kg N ha^{-1} yr^{-1}. Mean annual precipitation is 1400 mm and the mean annual temperature is 19 °C. The soil is calcareous with soil type being Cambisols on the slope and being Luvisols in the valley, underlain by a mixture of limestone and dolomite (Qian et al., 2023). The soil depth varied between the valley and the slope, being around 80 cm in the valley and around 30 cm on the slope. In the karst region, the underground conduit systems are very developed with the hydrological process being dominated by underground leakage vertically, and the overland flow or interflow being negligible (Fu et al., 2016).

An N addition experiment was established in the valley and on the slope to investigate whether the effect of N addition on soil C and N cycling would be mediated by topography (Fig. 1) (Wang et al., 2019). At each topographic position (i.e. slope or valley), a randomized block design was adopted with three replicated blocks and three N addition rates, including control (N0, 0 kg N ha^{-1} yr^{-1}), moderate N addition (N50, 50 kg N ha^{-1} yr^{-1}) and high N addition (N100, 100 kg N ha^{-1} yr^{-1}). This resulted in nine plots (10 m × 10 m each) at each topographic position. Each plot within a block was surrounded by a 10 m wide buffer zone. The shortest distance between the neighboring plots in the valley and on the slope was >30 m. During the application, NH_4NO_3 was dissolved in 10 L of water and sprayed with a back-pack sprayer to promote

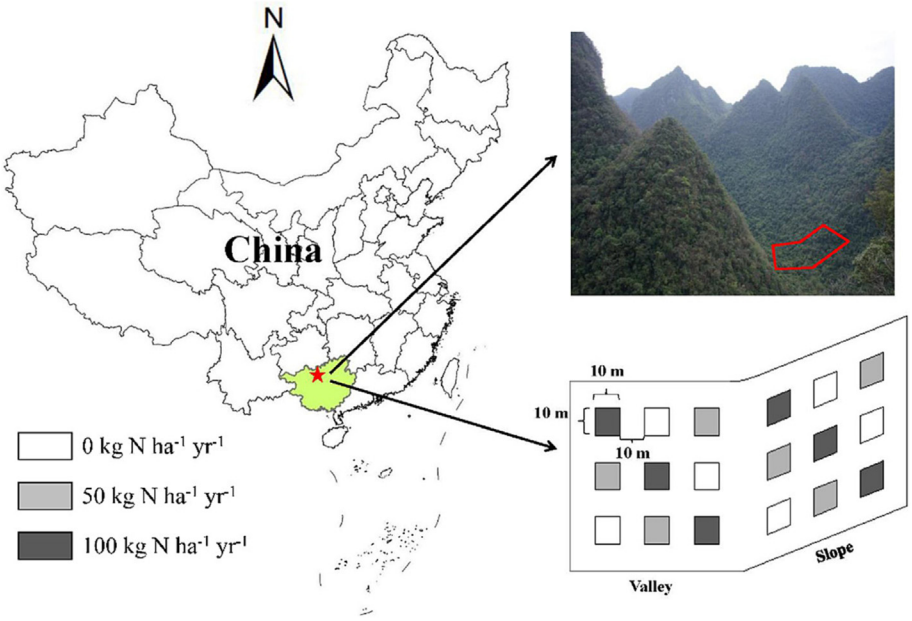

Fig. 1. Schematic map showing the experimental site and relative distribution of plots at two neighboring topographic positions. Figure derived from Wang et al. (2019).

an even distribution. Each control plot received 10 L water during each application. The N addition was carried out at the beginning of each month since April 2016.

2.2. Soil and litter sampling and physicochemical analyses

Two litter traps of 1 m × 1 m (~ 0.5 m above the forest floor) with a mesh size of 1 mm were deployed in each plot, with litterfall collected monthly since January 2017. The collected litter was dried in an oven at 60 °C for 48 h and weighed to calculate the cumulative litterfall production for each plot from January 2017 to September 2019.

Soil sampling was collected in September 2019. Three 20 cm × 20 cm locations were randomly selected in each plot. One soil core (0–10 cm) was collected from each location using a soil corer (5 cm in inner diameter) after removing litter. Fine roots (< 2 mm in diameter) and all attached residues (soil, dead roots, stem materials and litter fractions) were carefully removed by tweezers. The roots were then rinsed well in deionized water, dried in an oven at 60 °C for 48 h, and weighed to determine fine root biomass and element concentrations. Soil samples were sieved to 2 mm and divided into three parts. One part was stored at 4 °C for less than one week before measuring soil ammonium (NH_4^+), nitrite (NO_2^-) and nitrate (NO_3^-) concentrations, dissolved organic C and N (DOC and DON), microbial biomass C, N and P (MBC, MBN and MBP), microbial C metabolism, microbial N metabolism, and enzyme activities. The second part was air dried at room temperature for the analysis of soil pH, bulk SOC, total N (TN), total P (TP) and available P (AVP). The third part was stored at −20 °C for subsequent DNA extraction. Analyses of soil physicochemical variables were described in Duan et al. (2022a), and the data are presented in Table S1. The stoichiometric imbalance (SI) between available resources (DOC, total dissolved N and AVP) and soil microbial communities was calculated using Eq. (1) (Mooshammer et al., 2014):

$$SI_{X:Y} = \frac{X : Y_{resource}}{X : Y_{microbes}} \quad (1)$$

where the ratio of X:Y is C:N, C:P or N:P.

2.3. Gross N mineralization

The rate of gross N mineralization (GNM) was estimated using ^{15}N-isotope pool dilution technique, according to Li et al. (2017). To estimate GNM, duplicates of 4 g (dry weight equivalent) soil samples were weighed into polypropylene vials and pre-incubated at 60 % water hold capacity at 25 °C for one week. Then, 100 μL $^{15}NH_4NO_3$ (10 atom% ^{15}N) was added to each soil sample, before incubating at 25 °C. After pre-incubation, the formal soil incubation was terminated after 0.5 h (t0) and 24 h (t1), respectively, and soils were extracted with 20 mL of 2 M KCl. The NH_4^+-N contents in the extraction was determined using an auto–analyzer (FIAstar 5000, FOSS, Sweden). The ^{15}N-NH_4^+ in extraction was determined using the micro-diffusion method by a MAT 253 isotope-ratio mass spectrometer coupled with an FLASH2000HT elemental analyzer (Thermo Finnigan MAT, Bremen, Germany). The GNM rate (μg N g^{-1} h^{-1}) was calculated according to Eq. (2):

$$GNM = \frac{N_{t1} - N_{t0}}{t1 - t0} \times \frac{\ln\left(\frac{APE_{t0}}{APE_{t1}}\right)}{\ln\left(\frac{N_{t1}}{N_{t0}}\right)} \quad (2)$$

where N_{t0} and N_{t1} are NH_4^+-N contents at t0 and t1, respectively, and APE_{t0} and APE_{t1} denote the ^{15}N atom percent excess (%) in soil NH_4^+ at t0 and t1, respectively.

2.4. Microbial respiration, growth rate and element use efficiency

The short-term incubation experiment was conducted to determine microbial respiration and microbial growth using ^{18}O-H_2O (Spohn et al., 2016b). The soils were incubated at 60 % WHC, since this has been reported to be optimum for the simultaneous occurrence of nitrification and denitrification (Congreves et al., 2019) due to the uninhibited diffusion of both substrates and O_2 (Parton et al., 1996) and the occurrence of anaerobic microsites in soil matrix (Sexstone et al., 1985). We also chose an incubation temperature of 20 °C, as the region is located in the subtropical humid forest life zone with a monsoon climate, where the mean annual air temperature ranges from 17.8 to 22.2 °C. ^{18}O-H_2O was added to each soil in screw vials to reach an ^{18}O enrichment of 20 %. In a parallel set of control soil samples, the same volume of ^{16}O-H_2O was added. All soil samples were incubated for 24 h. Gas samples were collected after 24 h of incubation from the headspace of the vials for CO_2 determination using a gas chromatograph (Agilent GC 7890A, Agilent, USA). The soil samples were then frozen at −80 °C for DNA extraction using the DNeasy PowerSoil® Pro kit (MoBio Laboratories, Carlsbad, CA, USA), following the manufacturers' instructions. The ^{18}O abundance and total O content of DNA were

measured using a MAT 253 isotope-ratio mass spectrometer coupled with an FLASH2000HT elemental analyzer (Thermo Finnigan MAT, Bremen, Germany). Microbial C and N growth rates were calculated from the production of DNA during the soil incubation (Spohn et al., 2016b; Zheng et al., 2019). The DNA production ($DNA_{produced}$, μg) was calculated based on the variation in ^{18}O-DNA between labeled and unlabeled soil samples as Eq. (3):

$$DNA_{produced} = O_{total} \times \frac{at\%_{excess}}{100} \times \frac{100}{at\%_{label}} \times \frac{100}{31.21} \quad (3)$$

where O_{total} is the total O content of the dried DNA extract (μg O); $at.\%_{excess}$ is the at.% ^{18}O of the labeled sample minus the mean at.% ^{18}O of control samples. The average weight% of O in DNA is 31.21, according to the average formula ($C_{39}H_{44}O_{24}N_{15}P_4$). The specific $f_{DNA\text{-}C}$ and $f_{DNA\text{-}N}$ values were then applied to each soil sample replicate individually which multiplied by the DNA production rate, enabling the calculation of microbial C (μg C g^{-1} d^{-1}) and N (μg N g^{-1} d^{-1}) growth rates using Eqs. (4) and (5):

$$C_{growth} = \frac{f_{DNA-C} \times DNA_{produced}}{DW \times t} \quad (4)$$

$$N_{growth} = \frac{f_{DNA-N} \times DNA_{produced}}{DW \times t} \quad (5)$$

where DW is the soil dry mass and t is the incubation time in days. The $f_{DNA\text{-}C}$ was calculated for each specific sample to represent the ratio of soil MBC to soil DNA content while $f_{DNA\text{-}N}$ was calculated for each specific sample to represent the ratio of soil MBN to soil DNA content.

Microbial respiration rate (R_S, μg C g^{-1} d^{-1}) was calculated according to Eq. (6):

$$R_S = \frac{CO_2}{DW \times t} \times \frac{P_{re} \times n}{R \times T} \times V \quad (6)$$

where P_{re} is the atmosphere pressure (kPa); n is the molecular mass of the element C (12.01 g mol^{-1}); R is the ideal gas constant (8.314 J mol^{-1} K^{-1}); and T is the absolute temperature of the gas (295.15 K); V is the headspace volume (L) of the vials; CO_2 (ppm) is the CO_2 concentration produced during the 24 h incubation period.

Microbial CUE was determined by the ratio of C_{growth} over microbial C uptake ($C_{uptake} = C_{growth} + R_S$), and microbial NUE was determined by the ratio of N_{growth} over microbial N uptake ($N_{uptake} = N_{growth} + GNM$). Both CUE and NUE are dimensionless with a range from 0 to 1.

2.5. Activities of soil extracellular enzymes

The activities of C-acquiring (β–D–glucosidase; GB), N-acquiring (L–Leucine aminopeptidase; LAP and β–*N*–acetylglucosaminidase; NAG) and P–acquiring (acid phosphatase; AP) enzymes were determined fluorometrically following standard protocols (German et al., 2011). Detailed information about sample analyses and data is presented in Duan et al. (2022b). Microbial resource limitation was assessed using the vector length and angle, along with the stoichiometric ratios of extracellular enzyme activities (Moorhead et al., 2016). Higher vector length suggests a relatively higher C vs. nutrient limitation. Vector angle >45° indicates a relatively higher P vs. N limitation while angle <45° indicates a relatively higher N vs. P limitation. The calculations of vector length and angle are as Eqs. (7) and (8):

$$Vector\ length = \sqrt{(\ln BG/\ln(NAG + LAP))^2 + (\ln BG/\ln AP)^2} \quad (7)$$

$$Vector\ angle = Degrees(\text{atan2}(\ln BG/\ln AP), (\ln BG/\ln(NAG + LAP))) \quad (8)$$

2.6. Fungal and bacterial diversity and biomass

The diversity of bacterial and fungal communities were measured by amplifying the V3–V4 region of the 16S rRNA gene with primer pairs 338F/806R for bacteria, and the ITS gene with primers ITS1F/ITS2R for fungi (Liu et al., 2018). Bacterial and fungal α (richness) and β (community composition) diversity indexes were calculated based on 97 % OTU similarity of obtained bacterial and fungal sequences. Microbial composition was represented by the first component of nonmetric multidimensional scaling analysis (Wu et al., 2021). We also calculated the richness-to-biomass ratio (richness:biomass) for bacterial and fungal communities, respectively, as an index which shows where there is a high diversity relative to biomass, and vice versa (Bastida et al., 2021).

2.7. Statistical analysis

Two-way analysis of variance (ANOVA) was used to examine the main and interactive effects of N addition and topography on microbial CUE, NUE, growth rates, respiration rate, gross N mineralization, microbial diversity and biomass, as well as on the C, N and P stoichiometry of plants and soil. Independent sample *t*-tests were used to examine whether the difference was significant between the valley and slope for each N addition treatment. The effect was considered significant at $p < 0.05$ level. The above analyses were performed in SPSS 20.0 (IBM Co., Armonk, NY, USA). Data were tested for normality before analysis. Spearman correlation analysis was used to test the relationship among microbial CUE, NUE, growth rate, respiration rate, gross N mineralization, microbial diversity and biomass, enzyme activity, as well as soil and plant C, N and P concentrations and stoichiometry using packages *ggm* and *psych* in R version 4.1 (R Development Core Team, 2022).

Structural equation models (SEM) were established based on the theoretical model (Fig. S1), and were used to examine how microbial CUE and NUE were affected by abiotic (C, N and P stoichiometry of plants and soil) and biotic factors (fungal and bacterial community biomass, richness and diversity) under N addition in the valley and on the slope, respectively. Input variables were tested for multivariate normality and linearity. We firstly selected parameters significantly correlated with microbial CUE and NUE following Pearson correlation analysis to construct a basic model of N addition and topography regulation on microbial CUE and NUE. Then, all the possible models were tested to identify the optimum model using some parameters tested with maximum likelihood estimation. If necessary, variables were log transformed to mitigate departure from model assumptions. Model fitting criteria included Chi–square ($0 \le CHI/DF \le 3$), *P* value (> 0.05), root mean square error of approximation ($0 \le RMSEA \le 0.08$) and comparative fit index (CFI > 0.90). The SEM was constructed using AMOS 21.0 (Amos Development Corporation, Chicago, IL, USA).

3. Results

3.1. C, N and P stoichiometry of soil, microbial biomass and plant litter

In the valley, N addition resulted in significantly lower soil C:N, although there was no difference between N50 and N100 (Fig. 2a). Soil TDN:AVP was not affected by N50, but was significantly higher under N100 (Fig. 2f). On the slope, soil DOC:AVP (Fig. 2e), MBC:MBN (Fig. 2g), and $SI_{C:P}$ (Fig. 2k) were significantly lowered by N addition, but there was no significant difference between N50 and N100. Soil TDN:AVP (Fig. 2f) and $SI_{N:P}$ (Fig. 2i) were not affected by N50, but were significantly lower under N100 compared to the control (Fig. 2f). Soil MBC:MBP was significantly higher under N50, but was not affected by N100 (Fig. 2g). Soil C:P and N:P were significantly higher on the slope than in the valley under N100 (Fig. 2b, c). Soil DOC:AVP and TDN:AVP were significantly higher on the slope than in the valley under N0 or N50 (Fig. 2e, f). The $SI_{C:P}$ and $SI_{N:P}$ were significantly higher on the slope than in the valley under N0 (Fig. 2k, l).

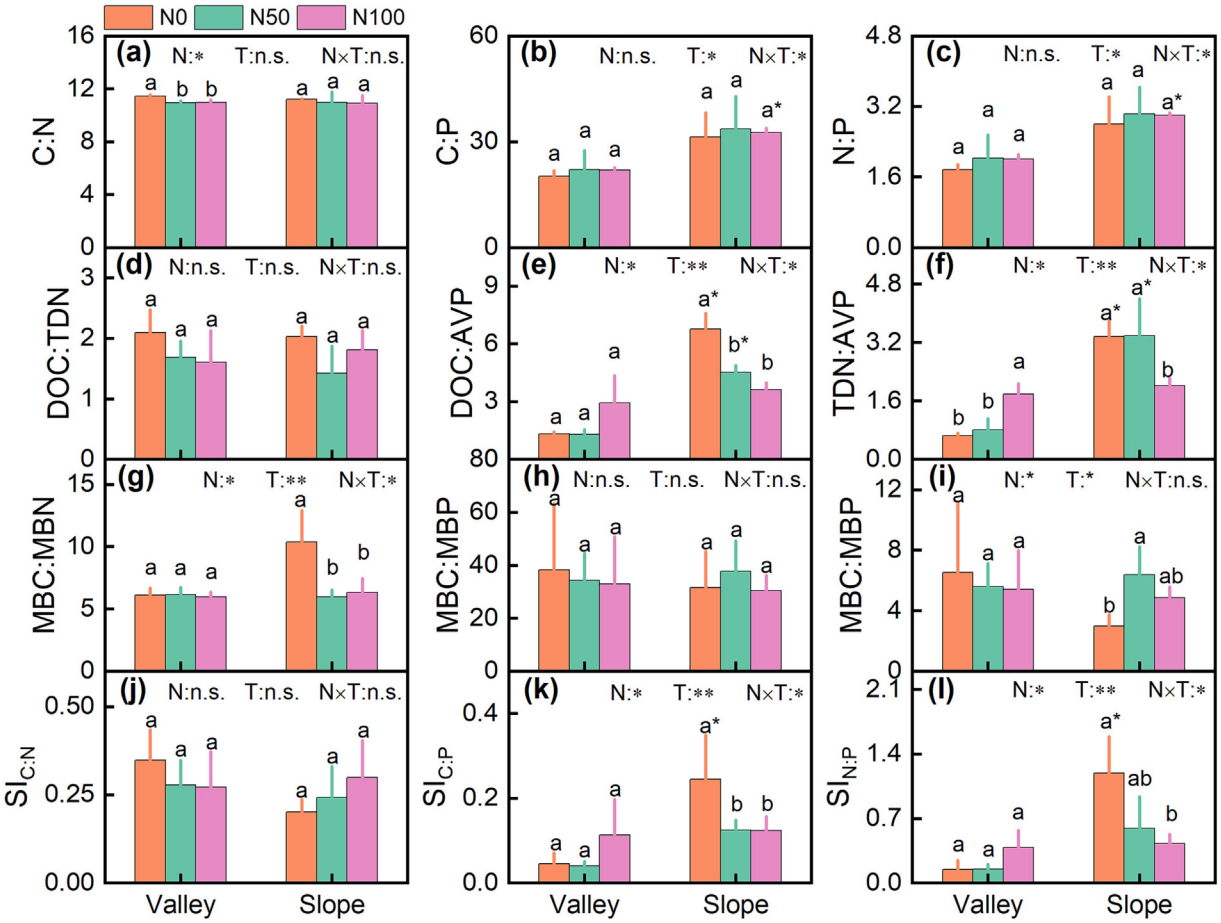

Fig. 2. The effect of N addition (N0, N50 and N100) on (a) C:N, (b) C:P, (c) N:P, (d) DOC:TDN, (e) DOC:AVP, (f) TDN:AVP, (g) MBC:MBN, (h) MBC:MBP, (i) MBN:MBP, (j) $SI_{C:N}$, (k) $SI_{C:P}$ and (d) $SI_{N:P}$ in the valley and on the slope. SI refers to the stoichiometric imbalance (see Materials and methods). Different letters denote significant difference at $p < 0.05$ among N addition treatments in the valley or on the slope, and * denotes significant difference at $p < 0.05$ between the valley and the slope. The p values from two-way ANOVA showing the effects of N addition (N), topography (T) and their interaction (N × T) are presented. *, $p < 0.05$; **, $p < 0.01$; ***, $p < 0.001$; n.s., not significant.

In the valley, litter C:N was significantly reduced by N addition with the values comparable between N50 and N100 (Fig. 3a). Root C:N was not affected by N50, but was significantly reduced by N100 (Fig. 3b). Root C:P and N:P were not affected by either level of N addition (Fig. 3c, d). In contrast, on the slope, litter C:N, root C:N and root N:P were not affected by N addition (Fig. 3a–c). However, root N:P was significantly higher under N50 but was not affected by N100 (Fig. 3d).

3.2. Stoichiometry between extracellular enzyme activities

In the valley, $E_{C:N}$ was significantly higher under N50 relative to N0 (Fig. 4a). The $E_{C:P}$ was significantly increased by N addition with the values comparable between N50 and N100 (Fig. 4b). However, N addition had no significant effect on $E_{N:P}$ (Fig. 4c). The N50 treatment significantly increased vector length, but N100 treatment had no significant effect on

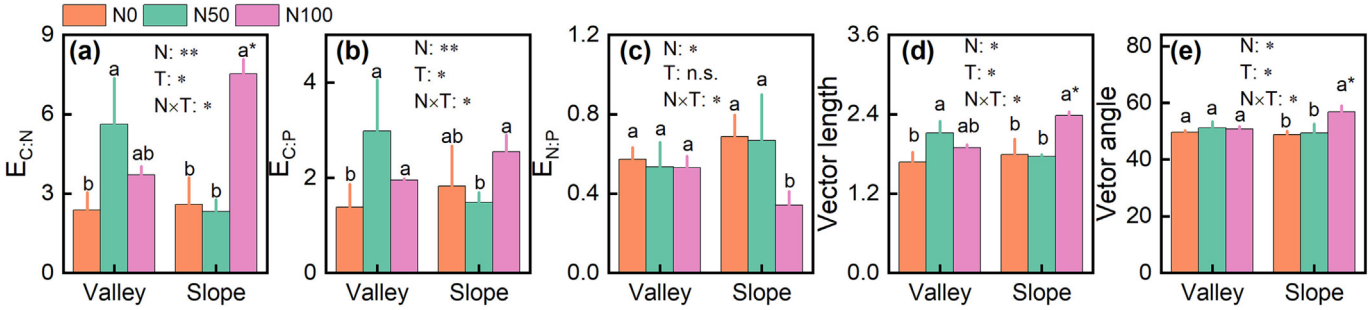

Fig. 3. Impacts of N addition on (a) $E_{C:N}$, (b) $E_{C:N}$, (c) $E_{C:N}$, (d) vector length and (e) vector angle in the valley and on the slope. [a]$E_{C:N}$, $E_{C:N}$ and $E_{C:N}$ represent stoichiometric ratios of C–, N– and P–acquiring ecoenzymes activities. [b]VL and VA represent vector length and vector angle. Different letters denote significant difference at $p < 0.05$ among N addition treatments in the valley or on the slope. Values are presented as means with standard deviations ($n = 3$). The p values from two-way ANOVA showing the effects of N addition (N), topography (T) and their interaction (N × T) are presented. *, $p < 0.05$; **, $p < 0.01$; ***, $p < 0.001$; n.s., not significant.

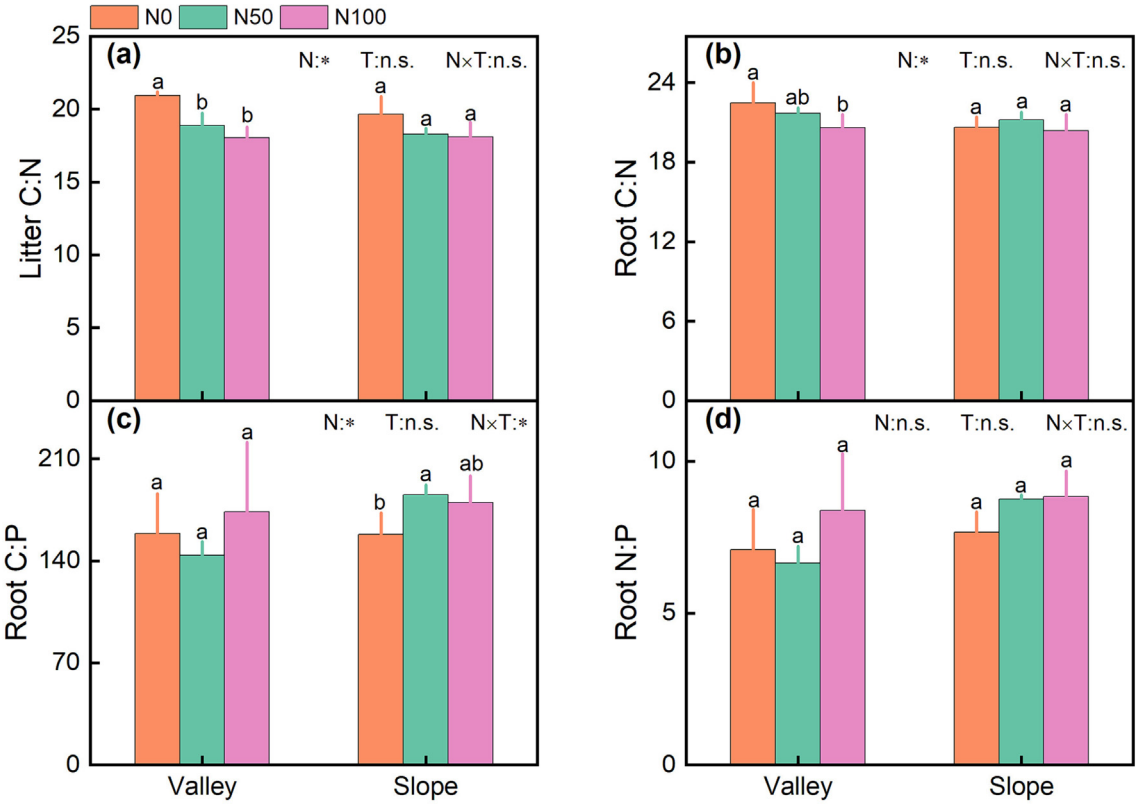

Fig. 4. Effect of N addition (N0, N50 and N100) on (a) litter C:N, (b) root C:N, (c) root C:P and (d) root N:P in the valley and on the slope. Different letters denote significant difference at $p < 0.05$ among N addition treatments in the valley or on the slope. The p values from two-way ANOVA showing the effects of N addition (N), topography (T) and their interaction (N × T) are presented. *, $p < 0.05$; **, $p < 0.01$; ***, $p < 0.001$; n.s., not significant.

vector length (Fig. 4d). The vector length was not affected by N addition (Fig. 4d).

On the slope, $E_{C:N}$ was similar under N0 and N50, but was significantly higher under N100 (Fig. 4a). Compared with N0, N50 and N100 did not significantly affect $E_{C:P}$, but $E_{C:P}$ was higher under N100 than N50 (Fig. 4b). The $E_{N:P}$ was not affected by N50, but was significantly lower under N100 compared to N0 (Fig. 4c). Vector length and angle were similar under N0 and N50, but were significantly higher under N100 (Fig. 4d, e).

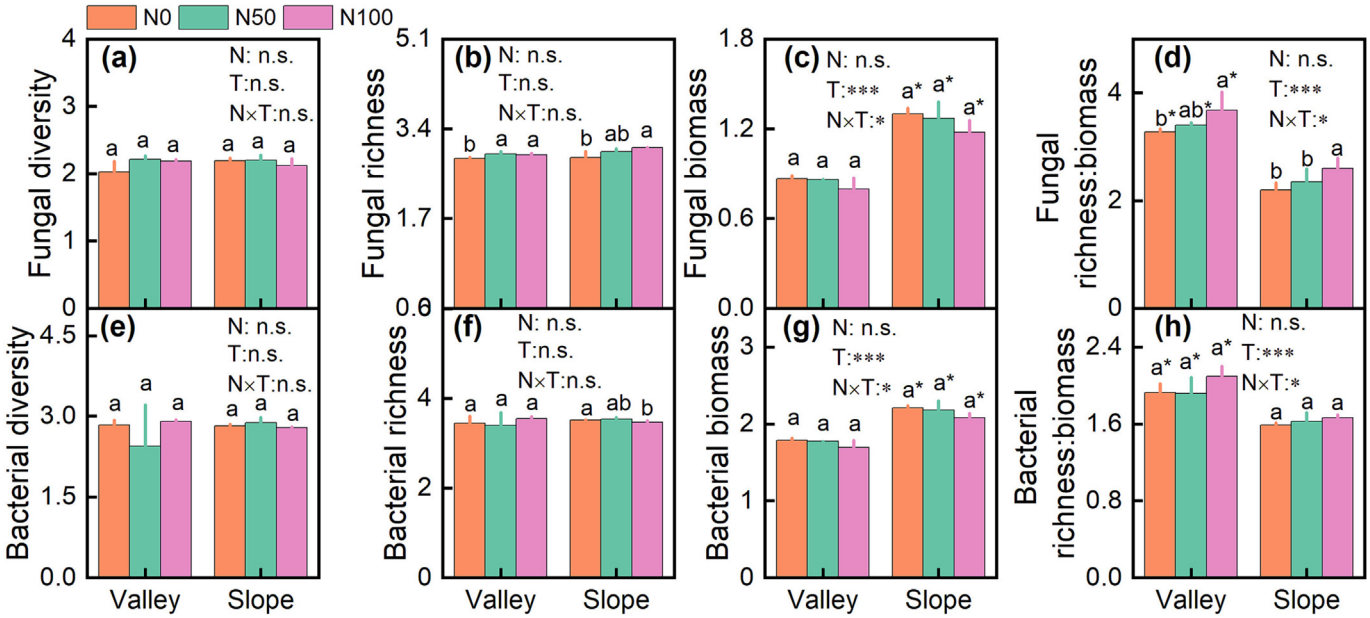

Fig. 5. Effect of N addition (N0, N50 and N100) on (a) fungal diversity, (b) fungal richness, (c) fungal biomass, (d) fungal richness:biomass, (e) bacterial diversity, (f) bacterial richness, (g) bacterial biomass and (h) bacterial richness:biomass in the valley and on the slope. Different letters denote significant difference at $p < 0.05$ among N addition treatments in the valley or on the slope, and * denotes significant difference at $p < 0.05$ between the valley and the slope. The p values from two-way ANOVA showing the effects of N addition (N), topography (T) and their interaction (N × T) are presented. *, $p < 0.05$; **, $p < 0.01$; ***, $p < 0.001$; n.s., not significant.

Both vector length and angle were significantly higher on the slope than in the valley under N100 (Fig. 4d, e).

3.3. Microbial diversity, richness and biomass

In the valley, N addition had no significant effects on fungal diversity and biomass, or bacterial diversity, richness, biomass and bacterial richness: biomass ratio (Fig. 5). Fungal richness was significantly increased by N addition with the values comparable between N50 and N100 (Fig. 5b). The ratio of fungal richness:biomass was similar under N0 and N50, but was significantly higher under N100 (Fig. 5d). On the slope, N addition had no significant effects on fungal diversity and biomass, or bacterial diversity, biomass and bacterial richness: biomass ratio (Fig. 5). Fungal richness and richness:biomass were not affected by N50, but were significantly higher under N100 compared to N0 (Fig. 5b, d). Bacterial richness was not affected by N50, but was significantly lowered by N100 (Fig. 5f). Fungal and bacterial biomass were significantly higher on the slope than in the valley regardless of N addition (Fig. 5c, g). Fungal and bacterial richness: biomass were significantly higher in the valley than on the slope irrespective of N addition (Fig. 5d, h).

3.4. Effect of nitrogen addition and topography on microbial carbon and nitrogen use efficiencies

Nitrogen addition had a significant effect on microbial CUE, while topography significantly affected microbial C growth and CUE (Table S3). There was a significant interactive effect of topography × N addition on microbial respiration or CUE (Table S3). Under N0, microbial C growth, respiration and CUE were 2.9 ± 0.6 μg C g^{-1} d^{-1}, 16.9 ± 2.8 μg C g^{-1} d^{-1} and 0.14 ± 0.01, on average, in the valley and 13.3 ± 3.0 μg C g^{-1} d^{-1}, 68.8 ± 37.6 μg C g^{-1} d^{-1} and 0.18 ± 0.06 on the slope (Fig. 6a–c). In the valley, N50 and N100 by 120 % and 420 %, respectively, compared to N0 (Fig. 6a). Microbial respiration rate was not significantly affected by N50, but was significantly increased by N100 by ca. 165 % compared to N0 (Fig. 6b). Microbial CUE was significantly increased by ca. 35 % and 90 %, respectively, by N50 and N100 relative to N0 (Fig. 6c). On the slope, microbial C growth and respiration rates were not significantly affected by N addition, but microbial CUE was increased by ca. 130 % and110%, respectively, by N50 and N100 compared to N0 (Fig. 6c).

Nitrogen addition had a significant effect on microbial N growth and NUE, while topography significantly affected microbial N growth, gross N mineralization and NUE (Table S3). There were also a significant interactive effects of topography × N addition on microbial N growth, gross N mineralization and NUE (Table S3). Microbial N growth, gross N mineralization and NUE were 0.48 ± 0.10 μg N g^{-1} d^{-1}, 2.5 ± 0.4 μg N g^{-1} d^{-1} and 0.16 ± 0.03, on average, in the valley and 1.4 ± 0.7 μg N g^{-1} d^{-1}, 3.1 ± 0.8 μg N g^{-1} d^{-1} and 0.3 ± 0.1 on the slope under N0 (Fig. 6d–f). In the valley, microbial N growth rate was ca. 115 % higher under N50, and ca. 430 % higher under N100 compared to N0 (Fig. 6d). Gross N mineralization was increased by ca. 30 % and 45 %, respectively, by N50 and N100 relative to N0 (Fig. 6e). Microbial NUE was not significantly affected by N50, but was significantly increased by N100 by ca. 155 % than N0 (Fig. 6f). On the slope, microbial N growth rate was significantly increased by ca.125 % by N50, but was not significantly affected by N100 (Fig. 6d). Gross N mineralization was not significantly affected by N50, but was significantly lowered by 60 % by N100 relative to N0 (Fig. 6e). Microbial NUE was significantly increased by ca. 90 % and 120 %, respectively, by N50 and N100 (Fig. 6c).

Microbial N growth rates under N50 and N100 on the slope were significantly higher their counterparts in the valley (Fig. 6a). CUE and microbial N growth rate under N50 on the slope were significantly higher than their counterparts in the valley (Figs. 6c, d), but the contrast pattern was

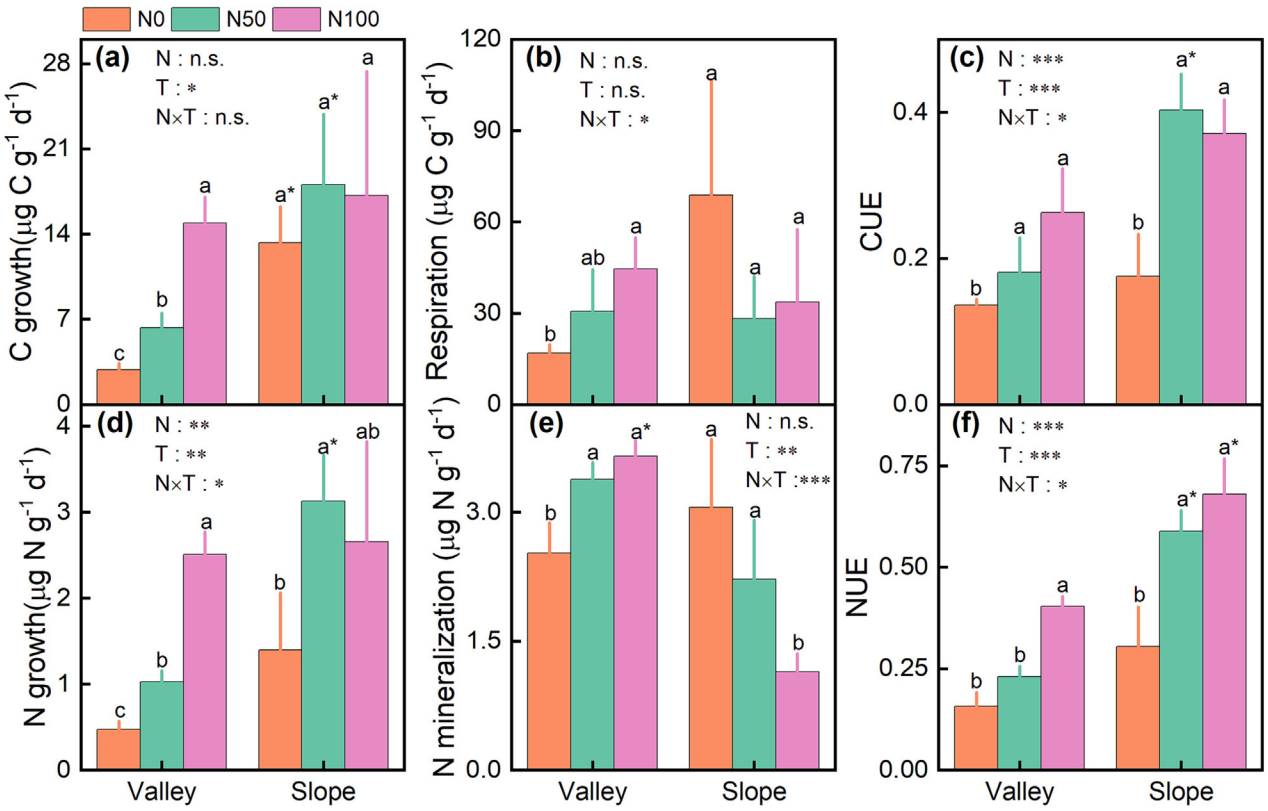

Fig. 6. Effect of N addition (N0, N50 and N100) on the rates of (a) microbial C growth, (b) respiration, (c) CUE, (d) microbial N growth, (e) gross N mineralization and (f) NUE in the valley and on the slope. Different letters denote significant difference at $p < 0.05$ among N addition treatments in the valley or on the slope, and * denotes significant difference at $p < 0.05$ between the valley and the slope. The p values from two-way ANOVA showing the effects of N addition (N), topography (T) and their interaction (N × T) are presented. *, $p < 0.05$; **, $p < 0.01$; ***, $p < 0.001$; n.s., not significant.

observed for N mineralization, with was significantly lower on the slope than in the valley under N100 (Fig. 6e).

3.5. Mechanisms underlying the impacts of nitrogen addition on microbial CUE and NUE

Based on SEM analyses, N addition increased microbial CUE by lowering litter C:N or increasing fungal richness:biomass with the model explaining 92 % of the variance of CUE in the valley (Fig. 7a). In contrast, N addition CUE via lowering soil DOC:AVP or microbial respiration, which was caused by decreased soil DOC:AVP or increased root N:P on the slope with the model explaining 78 % of the variance of CUE (Fig. 7c). NUE was increased by N addition due to increased microbial N growth caused by the stimulation of soil TDN:AVP and fungal richness: biomass by N addition in the valley (Fig. 7b). On the slope, N addition increased NUE owing to lowered gross N mineralization caused by decreased soil DOC:AVP (Fig. 7d). The models explained 86 % and 64 % of the variances of NUE in the valley and on the slope, respectively.

4. Discussion

4.1. Microbial carbon and nitrogen use efficiencies in the valley and on the slope

Our results show that microbial CUE under N0 was similar at both topographic positions (Fig. 6c). Although microbial C growth was significantly lower in the valley than on the slope under N0 (Fig. 5a), this did not result

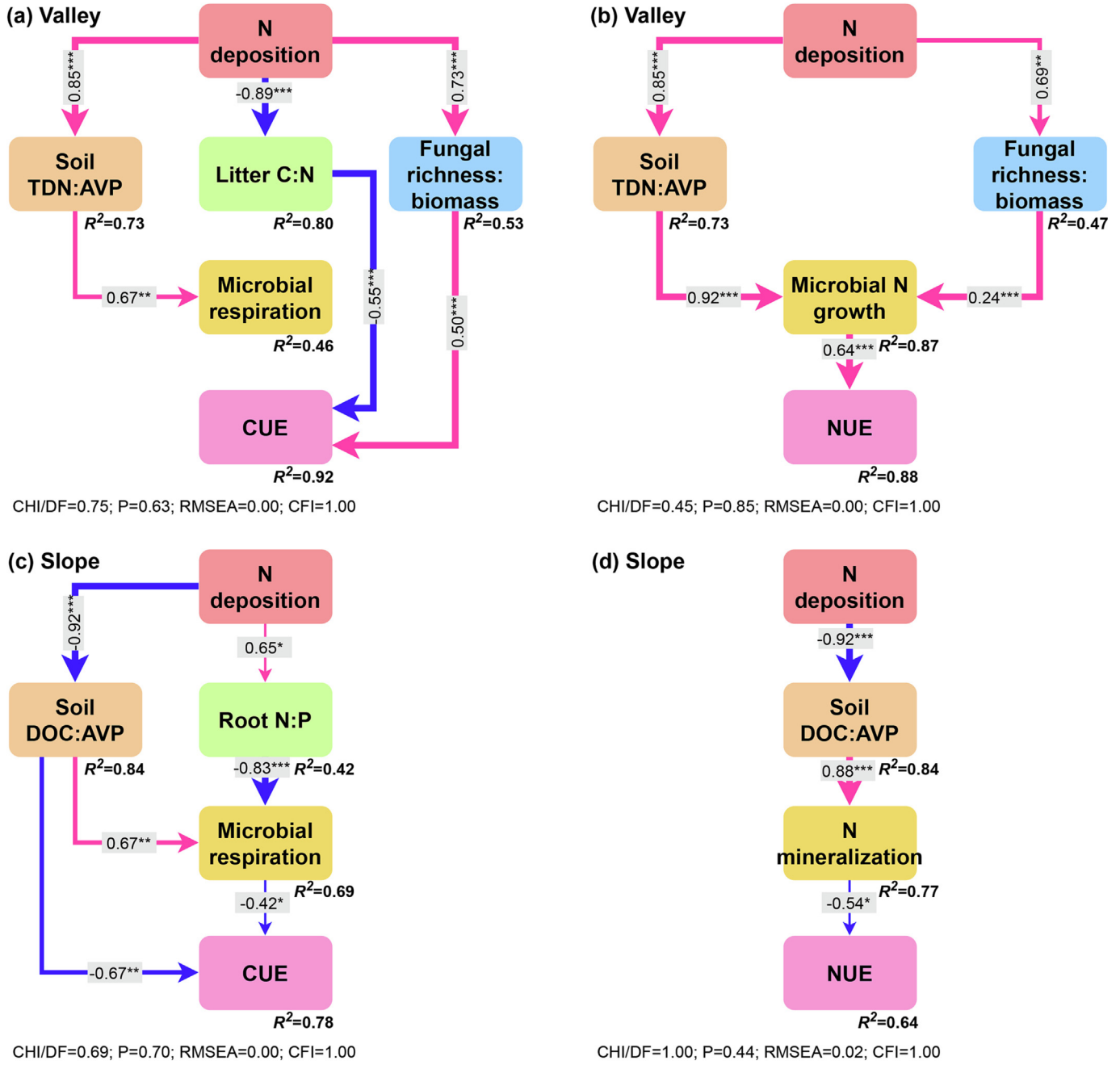

Fig. 7. Structural equation models (SEM) showing the influence of N addition on microbial CUE and NUE via soil and plant element stoichiometric ratios, microbial community traits, respiration, growth, and gross N mineralization in soils from the valley and the slope. The blue lines represent significant negative relationships and the pink lines represent significant positive relationships. Width of arrows represents the strength of the relationships. Numbers beside the lines are standardized path coefficients with asterisks indicating their significance (*$p < 0.05$, ** $p < 0.01$, *** $p < 0.001$).

in a lower CUE in the valley. Rather than reducing their CUE to help acquire C (Calabrese et al., 2022), microorganisms in the valley therefore appeared to cope with the lower C availability (Table S2) by reducing their growth rate but maintaining a relatively constant CUE (Spohn et al., 2016a). We also found that the vector length and angle had similar values under N0 at both topographic positions (Fig. 4d, e). This indicated that despite the lower availability of DOC in the valley soils, microbial C limitation was similar at the two topographic positions.

Our results also showed that microbial NUE for the N0 treatment were similar at both topographic positions. In the studied soils, the TDN concentration was higher under N0 on the slope than in the valley (Table S1; Duan et al., 2022a). However, microbial N growth, gross N mineralization and NUE were very similar under N0 at both positions (Fig. 6d–f). This finding therefore contrasted with several previous studies, where higher soil N availability has been associated with higher microbial NUE (Mooshammer et al., 2014; Wild et al., 2015). We also calculated the C/N ratio of substrates in the soil and found that there was no significant difference in SOC:TN (11.5 ± 0.1 v.s. 11.2 ± 0.1) and DOC:TDN (2.1 ± 0.4 v.s. 2.0 ± 0.2) between the valley and the slope. Based on microbial resource requirements, microbes are expected to increase their NUE when using substrate with a higher C:N ratio (Mooshammer et al., 2014). The similar ratio of C:N in the soils may therefore explain the very similar NUE at the two positions, despite differences in the total availability of TDN.

We found that microbial C and N metabolism after N addition in the field were significantly affected by topography. As mentioned above, higher microbial CUE and NUE have been previously associated with a higher availability of C and N in soil (Mooshammer et al., 2014; Wild et al., 2015). In the studied soils, although there was no difference in soil DOC and TDN concentrations between the slope and valley under the N50 treatment, the DOC:AVP and TDN:AVP were significantly higher on the slope than in the valley (Table S2). The lower DOC:AVP and TDN:AVP under N50 addition in the valley were attributed to the higher AVP concentration (Table S2). Increased gross N mineralization rate under N50 addition may release more available P in the valley, although mineralization rate was not significantly higher under N50 in the valley than on the slope (Fig. 6e). Moreover, greater microbial biomass C has been associated with a higher microbial NUE (Zhang et al., 2019). Consistent with this, we found that MBC, fungal and bacterial biomass with the N100 treatment were significantly higher on the slope than in the valley (Table S2, Fig. 5c, g). Thus, the higher microbial biomass under N100 treatment may have contributed to the higher microbial NUE on the slope (Fig. 6f). Together, these differences in microbial responses to N addition between the valley and slope suggest that topography regulated microbial CUE and NUE by differently influencing the stoichiometry of soil C, N and P and microbial biomass in the studied forest soils.

4.2. Mechanisms underlying the increase in microbial carbon use efficiency following N addition are topography-dependent

We find that N addition increased microbial CUE in the studied karst forests regardless of topographic position, which was consistent with our first hypothesis. This was also in line with some earlier studies, which reported that N addition increased microbial CUE in grassland, agricultural and forest ecosystems (Thiet et al., 2006; Poeplau et al., 2019; Morris et al., 2022). In agricultural soils, the long-term application of N fertilizer was found to increase microbial CUE by increasing the microbial C growth rate (Feng et al., 2022), while in a grassland soil N addition increased microbial CUE by reducing microbial respiration (Yuan et al., 2019). In our study, microbial C growth rate increased significantly under N addition in the valley, but had no significant effect on the slope (Fig. 6a). The contrasting responses of microbial C growth rate to N addition between the two topographic positions may be due to soil N content and availability (Manzoni et al., 2012; Feng et al., 2022). Under high N conditions, microorganisms may allocate more C to biomass synthesis (Manzoni and Porporato, 2009), thereby increasing microbial C growth rate and CUE. We also observed that TDN concentration increased significantly after N addition (Table S2) and this was positively correlated with microbial C growth (Fig. S2a) in the valley, contributing to the higher CUE. In contrast, microbial respiration was significantly increased under the N100 addition in the valley, but was not significantly impacted on the slope (Fig. 6b). The availability of soil C, nutrients and C:N:P stoichiometry under N addition were identified as key factors driving microbial respiration in grassland and forest ecosystems (Yuan et al., 2019; Eastman et al., 2021; Ning et al., 2021). Previous studies have also demonstrated that microbial CUE decreased with increasing soil C:N (Manzoni et al., 2012; Li et al., 2015), because the more stoichiometrically balanced substrate promoted microbial growth (Cheng et al., 2014) while excessive C is released through overflow respiration (Roller and Schmidt, 2015; Zang et al., 2016). Our data indicated that N addition elevated soil TDN concentration but reduced soil C:N in the valley (Table S2), suggesting that both substrate availability and stoichiometry contributed to the increased microbial respiration in the valley after N addition. The results of the enzymatic stoichiometry showed that vector length significantly increased under N50 in the valley (Fig. 4d), indicating a stronger microbial C limitation caused by N addition. This response further demonstrates that shifts in resource availability can alter microbial resource demands, with consequences for the efficiency of microbial resource use.

Our results also revealed an important role for plant-mediated changes in CUE, driven by changes in litter stoichiometry under N addition, with the effects differing between the valley and the slope (Fig. 7a, c). We observed that N addition elevated microbial CUE by reducing the C:N ratio of litter in the valley (Fig. 7a). The lower metabolic costs associated with N acquisition when the C:N stoichiometry of litter substrate is favorable may enable microorganisms to allocate more C to growth (Spohn et al., 2016a). In addition, a more stoichiometrically balanced resource will mean than less CO_2 is lost via overflow respiration, thus contributing to a higher CUE (Roller and Schmidt, 2015). In contrast with the valley, N addition on the slope increased the ratio of N:P in roots, which reduced respiration and increased CUE (Fig. 7c). It has been reported that the function of roots shifts from nutrient absorption to nutrient transport via increasing fine root biomass but decreasing root N:P ratio under N addition (Ostonen et al., 2017; Zhu et al., 2020). In our previous study, fine root biomass increased significantly under N100 addition on the slope (Yang et al., 2023), suggesting the shift in P may allocation from fine roots to leaves under increased N input. Therefore, the increased uptake of P by plants may have further aggravated soil microbial P limitation and thus inhibited microbial activity, resulting in lower microbial respiration on the slope. Although N addition did not significantly affect root N:P on the slope (Fig. 3d), N50 addition significantly increased root C:P (Fig. 3c), indicating that N addition had a negative effect on root P content. Phosphorus is an important component of cells and ATP, and can therefore regulate microbial growth and functions (Allen and Gillooly, 2009; Macdonald et al., 2018). As a result, the reduced P content of substrate may have constrained microbial respiration, and therefore promoted a higher CUE on the slope.

In the valley, N addition also appeared to regulate microbial CUE through impacting the microbial community composition (Fig. 7a). Nitrogen addition has often been shown to affect microbial community diversity and biomass (Bonner et al., 2018; Zhang et al., 2018), and these changes in the microbial community could impact microbial CUE (Domeignoz-Horta et al., 2020; Pold et al., 2020; Gavazov et al., 2022). A meta-analysis reported that a higher fungal richness:biomass was accompanied by a lower microbial respiration rate in soil (Bastida et al., 2021). These results suggested that fungal richess: biomass increased in the valley after N addition (Fig. 5d), indicating that higher fungal richness:biomass promoted higher microbial C growth relative to respiration, and therefore increased CUE. This may be because fungi communities are dominant in secreting enzymes that degrade organic matter, which would benefit microbial growth (Bonner et al., 2018).

4.3. Mechanisms underlying the increase in microbial nitrogen use efficiency following N addition are topography-dependent

We found that N addition increased microbial NUE regardless of topographic position in the karst forest, which was contrary to our second

hypothesis that N addition would decrease microbial NUE in the valley. A recent study demonstrated that N addition elevated microbial NUE in the mineral layer of a forest soil, with the higher microbial NUE accompanied by a higher microbial N growth rate and reduced gross N mineralization (Li et al., 2021b). Here, we found that N addition increased microbial N uptake for growth at both locations, but that N addition reduced gross N mineralization on the slope and increased it in the valley (Fig. 6d–f). Microbial N uptake is expected to increase with the increasing N availability in substrate (Wild et al., 2015). We observed that the N100 treatment significantly elevated soil TDN concentration and TDN:AVP in the valley (Table S2). Thus, a higher availability of N likely supported the higher microbial N growth rate, contributing to the increase NUE in the valley. Litter N content was positively related with microbial N growth rate on the slope (Fig. S2b), suggesting that elevated plant-derived N also supported enhanced microbial N growth. Changes in gross N mineralization can reflect a relative C or nutrients imbalance to microbial growth, which may be helpful in assessing the decoupling of organic N uptake and practical N demand (Zhang et al., 2019). Microorganisms mineralize organic compounds containing C and N for growth and energy metabolism under C limitation (Spohn et al., 2016b). In our study, the N50 addition significantly increased vector length in the valley (Fig. 4a), indicating that the N addition strengthened microbial C limitation. In the SEM, microbial N growth rate was also significantly and positively correlated with NUE in the valley (Fig. 7b). Together these results suggest that microbial C limitation induced by the added N could explain the increase in microbial N growth and gross N mineralization in the valley. Microbial NUE is defined by the balance between microbial growth and gross N mineralization, whereby a change in either or both processes generate a change in NUE (Zhang et al., 2019). Our results showed that gross N mineralization was negatively correlated with microbial NUE on the slope (Fig. 7d). Microbial NUE plays a central role in modulating the partitioning of organic N between anabolic and catabolic processes. On the slope, the gross N mineralization rate reduced after N addition, indicating that the reduced catabolic processes increased the NUE.

It has been shown that stoichiometric imbalance is important in regulating microbial N growth, mineralization and microbial NUE after N addition (Li et al., 2021b). The imbalance of N:P ratio between the dissolved soil fraction and microbial biomass can also explain differences in microbial NUE (Wild et al., 2015). In our study, $SI_{N:P}$ was positively correlated with microbial NUE in the valley but was negatively correlated with microbial NUE on the slope (Fig. S2). These results suggest that more AVP could promote microbial NUE on the slope, as microorganisms may be more constrained by soil P status on the slope, such that a higher availability of P may be beneficial for microbial N assimilation (Wu et al., 2022). In the SEM, N addition increased microbial NUE by increasing soil TDN:AVP and microbial N growth rate in the valley (Fig. 7b), and increasing microbial NUE by decreasing soil DOC:AVP and gross N mineralization on the slope (Fig. 7d). Similar to microbial CUE, soil total and available P contents were not clearly associated with to microbial C and N metabolism, but the stoichiometric ratios of available P strongly modulated microbial C and N metabolism.

Our findings showed that N100 addition significantly increased fungal richness:biomass at both topographic positions (Fig. 5d), and this ratio was positively associated with microbial NUE (Fig. S2). This suggested that fungal soil communities were sensitive to N-rich conditions and were the primary regulator of microbial NUE in our study. In contrast with this, a previous study reported that bacterial communities played a key role in modulating microbial NUE after N addition (Li et al., 2021b). Different microbial strains may vary in their N metabolism (Kamble and Bååth, 2016; Cheng et al., 2017), thereby shifts in community compositions under N addition could affect microbial NUE and therefore impact important ecosystem functions, including mineralization and denitrification. On the other hand, the fungal communities are often associated with slow element turnover, resulting in higher N accumulation and retention within the ecosystem (Ren et al., 2023). The results from our study further suggest that fungal communities may be important in contributing to N retention within soil, due to their higher NUE. In conclusion, these results revealed an empirical link between the microbial NUE and community, which could help explain the interrelation between microbial community and soil N retention (de Vries et al., 2012).

5. Conclusions

In the studied subtropical forest, N addition typically increased microbial CUE and NUE both in the valley and on the slope. However, the mechanisms underlying the responses of microbial CUE and NUE to N addition differed between the topographic positions. Variation in the soil C, N and P stoichiometric ratio and microbial biomass were the main explanatory factors accounting for the difference in microbial CUE and NUE between two topographic positions. The increase in CUE was associated with higher soil fungal richness:biomass and a lower litter C:N in the valley, whereas was linked with a reduced DOC:AVP ratio or with reduced microbial respiration caused by the lowered soil DOC:AVP and increased root N:P ratios on the slope. The increase in NUE was explained by stimulated microbial N growth relative to gross N mineralization caused by increased ratios of soil TDN:AVP and fungal richness:biomass ratios in the valley, but was attributed to decreased gross N mineralization caused by increased DOC:AVP ratio on the slope. As such, these results suggest that topography-driven differences in microbial communities and the stoichiometry of available C, N and P should be integrated into Earth system models in order to better predict microbial C and N metabolism under elevated atmospheric N deposition.

CRediT authorship contribution statement

Xinyi Yang: Conceptualization, Methodology, Formal analysis, Writing – original draft;
Pengpeng Duan: Investigation, Visualization, Validation, Methodology;
Lettice Hicks: Review & editing;
Kelin Wang: Conceptualization; Supervision
Dejun Li: Conceptualization, Methodology, Funding acquisition, Writing – review & editing.

Data availability

Data will be made available on request.

Declaration of competing interest

The authors declare that they have no known competing financial interests or personal relationships that could have appeared to influence the work reported in this paper.

Acknowledgements

This work was funded by the National Natural Science Foundation of China (U21A2007, 42107381 and 32001175), the Guangxi Bagui Scholarship Program to Dejun Li, and the Special Research Assistant Fellowship of Chinese Academy of Sciences to Xinyi Yang.

Appendix A. Supplementary data

Supplementary data to this article can be found online at https://doi.org/10.1016/j.scitotenv.2023.163236.

References

Allen, A.P., Gillooly, J.F., 2009. Towards an integration of ecological stoichiometry and the metabolic theory of ecology to better understand nutrient cycling. Ecol. Lett. 12, 369–384.
Bastida, F., Eldridge, D.J., García, C., Kenny Png, G., Bardgett, R.D., Delgado-Baquerizo, M., 2021. Soil microbial diversity–biomass relationships are driven by soil carbon content across global biomes. ISME J. 15, 2081–2091.
Bonner, M.T.L., Shoo, L.P., Brackin, R., Schmidt, S., 2018. Relationship between microbial composition and substrate use efficiency in a tropical soil. Geoderma 315, 96–103.

Buckeridge, K.M., La Rosa, A.F., Mason, K.E., Whitaker, J., McNamara, N.P., Grant, H.K., Ostle, N.J., 2020. Sticky dead microbes: rapid abiotic retention of microbial necromass in soil. Soil Biol. Biochem. 149, 107929.
Calabrese, S., Mohanty, B.P., Malik, A.A., 2022. Soil microorganisms regulate extracellular enzyme production to maximize their growth rate. Biogeochemistry 158, 303–312.
Cheng, W., Parton, W.J., Gonzalez-Meler, M.A., Phillips, R., Asao, S., McNickle, G.G., Brzostek, E., Jastrow, J.D., 2014. Synthesis and modeling perspectives of rhizosphere priming. New Phytol. 201, 31–44.
Cheng, Y., Wang, J., Wang, J., Chang, S.X., Wang, S., 2017. The quality and quantity of exogenous organic carbon input control microbial NO3− immobilization: a meta–analysis. Soil Biol. Biochem. 115, 357–363.
Congreves, K.A., Phan, T., Farrell, R.E., 2019. A new look at an old concept: using 15N2O isotopomers to understand the relationship between soil moisture and N2O production pathways. Soil 5, 265–274.
de Vries, F.T., Bloem, J., Quirk, H., Stevens, C.J., Bol, R., Bardgett, R.D., 2012. Extensive management promotes plant and microbial nitrogen retention in temperate grassland. PLoS One 7, e51201.
Domeignoz-Horta, L.A., Pold, G., Liu, X.J.A., Frey, S.D., Melillo, J.M., DeAngelis, K.M., 2020. Microbial diversity drives carbon use efficiency in a model soil. Nat. Commun. 11, 3684.
Du, Z., Riveros-Iregui, D.A., Jones, R.T., McDermott, T.R., Dore, J.E., McGlynn, B.L., Emanuel, R.E., Li, X., 2015. Landscape position influences microbial composition and function via redistribution of soil water across a watershed. Appl. Environ. Microbiol. 81, 8457–8468.
Duan, P., Wang, D., Xiao, K., Zheng, L., Chen, H., Wang, K., Li, D., 2022a. Responses of soil nitrous oxide emission to nitrogen addition at two topographic positions of a subtropical Forest. J. Geophys. Res. Biogeosci. 127, e2021JG006539.
Duan, P., Xiao, K., Jiang, Y., Li, D., 2022b. Mechanisms underlying the responses of soil N2O production by ammonia oxidizers to nitrogen addition are mediated by topography in a subtropical forest. Geoderma 425, 116036.
Duan, P., Yang, X., He, X., Jiang, Y., Xiao, K., Wang, K., Li, D., 2022c. Topography–driven soil properties modulate effects of nitrogen deposition on soil nitrous oxide sources in a subtropical forest. Biol. Fertil. Soils 58, 707–720.
Eastman, B.A., Adams, M.B., Brzostek, E.R., Burnham, M.B., Carrara, J.E., Kelly, C., McNeil, B.E., Walter, C.A., Peterjohn, W.T., 2021. Altered plant carbon partitioning enhanced forest ecosystem carbon storage after 25 years of nitrogen additions. New Phytol. 230, 1435–1448.
Enanga, E.M., Casson, N.J., Fairweather, T.A., Creed, I.F., 2017. Nitrous oxide and dinitrogen: the missing flux in nitrogen budgets of forested Catchments? Environ. Sci. Technol. 51, 6036–6043.
Fairbanks, D., Shepard, C., Murphy, M., Rasmussen, C., Chorover, J., Rich, V., Gallery, R., 2020. Depth and topographic controls on microbial activity in a recently burned sub–alpine catchment. Soil Biol. Biochem. 148, 107844.
Feng, J., Zeng, X.M., Zhang, Q., Zhou, X.Q., Liu, Y.R., Huang, Q., 2021. Soil microbial trait–based strategies drive metabolic efficiency along an altitude gradient. ISME Commun. 1, 71.
Feng, X., Qin, S., Zhang, D., Chen, P., Hu, J., Wang, G., Liu, Y., Wei, B., Li, Q., Yang, Y., Chen, L., 2022. Nitrogen input enhances microbial carbon use efficiency by altering plant–microbe–mineral interactions. Glob. Chang. Biol. 28, 4845–4860.
Fu, Z., Chen, H., Xu, Q., Jia, J., Wang, S., Wang, K., 2016. Role of epikarst in near-surface hydrological processes in a soil mantled subtropical dolomite karst slope: implications of field rainfall simulation experiments. Hydrol. Process. 30, 795–811.
Fuchslueger, L., Wild, B., Mooshammer, M., Takriti, M., Kienzl, S., Knoltsch, A., Hofhansl, F., Bahn, M., Richter, A., 2019. Microbial carbon and nitrogen cycling responses to drought and temperature in differently managed mountain grasslands. Soil Biol. Biochem. 135, 144–153.
Gavazov, K., Canarini, A., Jassey, V.E.J., Mills, R., Richter, A., Sundqvist, M.K., Väisänen, M., Walker, T.W.N., Wardle, D.A., Dorrepaal, E., 2022. Plant–microbial linkages underpin carbon sequestration in contrasting mountain tundra vegetation types. Soil Biol. Biochem. 165, 108530.
German, D.P., Weintraub, M.N., Grandy, A.S., Lauber, C.L., Rinkes, Z.L., Allison, S.D., 2011. Optimization of hydrolytic and oxidative enzyme methods for ecosystem studies. Soil Biol. Biochem. 43, 1387–1397.
Hasby, F.A., Barbi, F., Manzoni, S., Lindahl, B.D., 2021. Transcriptomic markers of fungal growth, respiration and carbon–use efficiency. FEMS Microbiol. Lett. 368.
Kamble, P.N., Bååth, E., 2016. Comparison of fungal and bacterial growth after alleviating induced N–limitation in soil. Soil Biol. Biochem. 103, 97–105.
Keller, N., Bol, R., Herre, M., Marschner, B., Heinze, S., 2023. Catchment scale spatial distribution of soil enzyme activities in a mountainous German coniferous forest. Soil Biol. Biochem. 177, 108885.
Li, W., Jin, C., Guan, D., Wang, Q., Wang, A., Yuan, F., Wu, J., 2015. The effects of simulated nitrogen deposition on plant root traits: a meta–analysis. Soil Biol. Biochem. 82, 112–118.
Li, D., Yang, Y., Chen, H., Xiao, K., Song, T., Wang, K., 2017. Soil gross nitrogen transformations in typical karst and nonkarst forests, Southwest China. J. Geophys. Res. Biogeosci. 122, 2831–2840.
Li, J., Pei, J., Dijkstra, F.A., Nie, M., Pendall, E., 2021a. Microbial carbon use efficiency, biomass residence time and temperature sensitivity across ecosystems and soil depths. Soil Biol. Biochem. 154, 108117.
Li, J., Sang, C., Yang, J., Qu, L., Xia, Z., Sun, H., Jiang, P., Wang, X., He, H., Wang, C., 2021b. Stoichiometric imbalance and microbial community regulate microbial elements use efficiencies under nitrogen addition. Soil Biol. Biochem. 156, 108207.
Liang, C., Schimel, J.P., Jastrow, J.D., 2017. The importance of anabolism in microbial control over soil carbon storage. Nat. Microbiol. 2, 17105.
Liu, Y.R., Delgado-Baquerizo, M., Wang, J.T., Hu, H.W., Yang, Z., He, J.Z., 2018. New insights into the role of microbial community composition in driving soil respiration rates. Soil Biol. Biochem. 118, 35–41.
Macdonald, C.A., Delgado-Baquerizo, M., Reay, D.S., Hicks, L.C., Singh, B.K., 2018. Chapter 6–Soil nutrients and soil carbon storage: modulators and mechanisms. In: Singh, B.K. (Ed.), Soil Carbon Storage. Academic Press, pp. 167–205.
Malik, A.A., Puissant, J., Buckeridge, K.M., Goodall, T., Jehmlich, N., Chowdhury, S., Gweon, H.S., Peyton, J.M., Mason, K.E., van Agtmaal, M., Blaud, A., Clark, I.M., Whitaker, J., Pywell, R.F., Ostle, N., Gleixner, G., Griffiths, R.I., 2018. Land use driven change in soil pH affects microbial carbon cycling processes. Nat. Commun. 9, 3591.
Manzoni, S., Porporato, A., 2009. Soil carbon and nitrogen mineralization: theory and models across scales. Soil Biol. Biochem. 41, 1355–1379.
Manzoni, S., Taylor, P., Richter, A., Porporato, A., Ågren, G.I., 2012. Environmental and stoichiometric controls on microbial carbon–use efficiency in soils. New Phytol. 196, 79–91.
Moorhead, D.L., Sinsabaugh, R.L., Hill, B.H., Weintraub, M.N., 2016. Vector analysis of ecoenzyme activities reveal constraints on coupled C, N and P dynamics. Soil Biol. Biochem. 93, 1–7.
Mooshammer, M., Wanek, W., Hämmerle, I., Fuchslueger, L., Hofhansl, F., Knoltsch, A., Schnecker, J., Takriti, M., Watzka, M., Wild, B., 2014. Adjustment of microbial nitrogen use efficiency to carbon: nitrogen imbalances regulates soil nitrogen cycling. Nat. Commun. 5, 3694.
Morris, K.A., Richter, A., Migliavacca, M., Schrumpf, M., 2022. Growth of soil microbes is not limited by the availability of nitrogen and phosphorus in a Mediterranean oak–savanna. Soil Biol. Biochem. 169, 108680.
Ning, Q., Hättenschwiler, S., Lü, X., Kardol, P., Zhang, Y., Wei, C., Xu, C., Huang, J., Li, A., Yang, J., Wang, J., Peng, Y., Peñuelas, J., Sardans, J., He, J., Xu, Z., Gao, Y., Han, X., 2021. Carbon limitation overrides acidification in mediating soil microbial activity to nitrogen enrichment in a temperate grassland. Glob. Chang. Biol. 27, 5976–5988.
Ostonen, I., Truu, M., Helmisaari, H.S., Lukac, M., Borken, W., Vanguelova, E., Godbold, D.L., Lõhmus, K., Zang, U., Tedersoo, L., Preem, J.K., Rosenvald, K., Aosaar, J., Armolaitis, K., Frey, J., Kabral, N., Kukumägi, M., Leppälammi-Kujansuu, J., Lindroos, A.J., Merilä, P., Napa, Ü., Nõjd, P., Parts, K., Uri, V., Varik, M., Truu, J., 2017. Adaptive root foraging strategies along a boreal–temperate forest gradient. New Phytol. 215, 977–991.
Parton, W., Mosier, A., Ojima, D., Valentine, D., Schimel, D., Weier, K., Kulmala, A.E., 1996. Generalized model for N2 and N2O production from nitrification and denitrification. Glob. Biogeochem. Cycles 10, 401–412.
Poeplau, C., Helfrich, M., Dechow, R., Szoboszlay, M., Tebbe, C.C., Don, A., Greiner, B., Zopf, D., Thumm, U., Korevaar, H., Geerts, R., 2019. Increased microbial anabolism contributes to soil carbon sequestration by mineral fertilization in temperate grasslands. Soil Biol. Biochem. 130, 167–176.
Pold, G., Domeignoz-Horta, L.A., Morrison, E.W., Frey, S.D., Sistla, S.A., DeAngelis, K.M., Giovannoni, S.J., 2020. Carbon use efficiency and its temperature sensitivity covary in soil bacteria. MBio 11 e02293-02219.
Preusser, S., Marhan, S., Poll, C., Kandeler, E., 2017. Microbial community response to changes in substrate availability and habitat conditions in a reciprocal subsoil transfer experiment. Soil Biol. Biochem. 105, 138–152.
Qian, Z., Gu, R., Gao, K., Li, D., 2023. High plant species diversity enhances lignin accumulation in a subtropical forest of Southwest China. Sci. Total Environ. 865, 161113.
Ren, G., Zhang, X., Xin, X., Yang, W., Zhu, A., Yang, J., Li, M., 2023. Soil organic carbon and nitrogen fractions as affected by straw and nitrogen management on the North China plain. Agric. Ecosyst. Environ. 342, 108248.
Roller, B.R.K., Schmidt, T.M., 2015. The physiology and ecological implications of efficient growth. ISME J. 9, 1481–1487.
Sexstone, A.J., Revsbech, N.P., Parkin, T.B., Tiedje, J.M., 1985. Direct measurement of oxygen profiles and denitrification rates in soil aggregates. Soil Sci. Soc. Am. J. 49, 645–651.
Smith, T.P., Clegg, T., Bell, T., Pawar, S., 2021. Systematic variation in the temperature dependence of bacterial carbon use efficiency. Ecol. Lett. 24, 2123–2133.
Spohn, M., Klaus, K., Wanek, W., Richter, A., 2016a. Microbial carbon use efficiency and biomass turnover times depending on soil depth–Implications for carbon cycling. Soil Biol. Biochem. 96, 74–81.
Spohn, M., Pötsch, E.M., Eichorst, S.A., Woebken, D., Wanek, W., Richter, A., 2016b. Soil microbial carbon use efficiency and biomass turnover in a long–term fertilization experiment in a temperate grassland. Soil Biol. Biochem. 97, 168–175.
Thiet, R.K., Frey, S.D., Six, J., 2006. Do growth yield efficiencies differ between soil microbial communities differing in fungal:bacterial ratios? Reality check and methodological issues. Soil Biol. Biochem. 38, 837–844.
Viscarra Rossel, R.A., Lee, J., Behrens, T., Luo, Z., Baldock, J., Richards, A., 2019. Continental-scale soil carbon composition and vulnerability modulated by regional environmental controls. Nat. Geosci. 12, 547–552.
Wang, Z., Li, D., Zheng, M., Chen, H., Sun, X., Wang, K., 2019. Topography modulates effects of nitrogen deposition on asymbiotic N2 fixation in soil but not litter or Moss in a secondary karst Forest. J. Geophys. Res. Biogeosci. 124, 3015–3023.
Wild, B., Schnecker, J., Knoltsch, A., Takriti, M., Mooshammer, M., Gentsch, N., Mikutta, R., Alves, R.J.E., Gittel, A., Lashchinskiy, N., Richter, A., 2015. Microbial nitrogen dynamics in organic and mineral soil horizons along a latitudinal transect in western Siberia. Glob. Biogeochem. Cycles 29, 567–582.
Wu, M.H., Chen, S.Y., Chen, J.W., Xue, K., Chen, S.L., Wang, X.M., Chen, T., Kang, S.C., Rui, J.P., Thies, J.E., Bardgett, R.D., Wang, Y.F., 2021. Reduced microbial stability in the active layer is associated with carbon loss under alpine permafrost degradation. Proc. Natl. Acad. Sci. 118, e2025321118.
Wu, W., Wang, F., Xia, A., Zhang, Z., Wang, Z., Wang, K., Dong, J., Li, T., Wu, Y., Che, R., Li, L., Niu, S., Hao, Y., Wang, Y., Cui, X., 2022. Meta–analysis of the impacts of phosphorus addition on soil microbes. Agric. Ecosyst. Environ. 340, 108180.
Yang, X., Duan, P., Wang, K., Li, D., 2023. Topography modulates effects of nitrogen deposition on soil nitrogen transformations by impacting soil properties in a subtropical forest. Geoderma 432, 116381.
Yuan, X., Niu, D., Gherardi, L.A., Liu, Y., Wang, Y., Elser, J.J., Fu, H., 2019. Linkages of stoichiometric imbalances to soil microbial respiration with increasing nitrogen addition: evidence from a long-term grassland experiment. Soil Biol. Biochem. 138, 107580.

Yuan, Z., Ali, A., Ruiz-Benito, P., Jucker, T., Mori, A.S., Wang, S., Zhang, X., Li, H., Hao, Z., Wang, X., Loreau, M., 2020. Above– and below–ground biodiversity jointly regulate temperate forest multifunctionality along a local–scale environmental gradient. J. Ecol. 108, 2012–2024.
Zang, H., Wang, J., Kuzyakov, Y., 2016. N fertilization decreases soil organic matter decomposition in the rhizosphere. Appl. Soil Ecol. 108, 47–53.
Zhang, T.A., Chen, H.Y.H., Ruan, H., 2018. Global negative effects of nitrogen deposition on soil microbes. ISME J. 12, 1817–1825.
Zhang, S., Zheng, Q., Noll, L., Hu, Y., Wanek, W., 2019. Environmental effects on soil microbial nitrogen use efficiency are controlled by allocation of organic nitrogen to microbial growth and regulate gross N mineralization. Soil Biol. Biochem. 135, 304–315.
Zhang, K., Chen, L., Li, Y., Brookes, P.C., Xu, J., Luo, Y., 2020. Interactive effects of soil pH and substrate quality on microbial utilization. Eur. J. Soil Biol. 96, 103151.
Zheng, Q., Hu, Y., Zhang, S., Noll, L., Böckle, T., Richter, A., Wanek, W., 2019. Growth explains microbial carbon use efficiency across soils differing in land use and geology. Soil Biol. Biochem. 128, 45–55.
Zhu, X., Liu, M., Kou, Y., Liu, D., Liu, Q., Zhang, Z., Jiang, Z., Yin, H., 2020. Differential effects of N addition on the stoichiometry of microbes and extracellular enzymes in the rhizosphere and bulk soils of an alpine shrubland. Plant Soil 449, 285–301.
Zhu, J., Jansen-Willems, A., Müller, C., Dörsch, P., 2021. Topographic differences in nitrogen cycling mediate nitrogen retention in a subtropical, N–saturated forest catchment. Soil Biol. Biochem. 159, 108303.